Simulations of Energetic Particle Driven Geodesic Acoustic Mode and Global Alfven Eigenmode in 3-dimensional LHD Equilibrium

H. Wang[1], Y. Todo[1,2] and Y. Suzuki[1,2]

[1]National Institute of Fusion Science, Toki, Japan
[2]The Graduate University for Advanced Studies, Toki, Japan

Corresponding Author: wanghao@nifs.ac.jp

Abstract:
Energetic particle driven geodesic acoustic mode (EGAM) in a 3-dimensional Large Helical Device (LHD) equilibrium are investigated using MEGA code. MEGA is a hybrid simulation code for energetic particles interacting with a magnetohydrodynamic (MHD) fluid. The poloidal velocity oscillation is a combination of $m/n = 0/0$ (strong), $1/0$ (medium) and $2/10$ (weak) components. This is caused by the LHD configuration, different from the tokamak case. The phenomena of chirping primary mode and the associated half-frequency secondary mode are firstly reproduced with the realistic input parameters and 3-dimensional equilibrium. There are good agreements between simulation and experiment on the frequency chirping of the primary mode, on the excitation of the half-frequency secondary mode, on the mode profile, and on the phase lock. It is found that the bulk pressure perturbation and the energetic particle pressure perturbation cancel out with each other, and thus the frequency of the secondary mode is lower than the primary mode. Also, it is found that the secondary mode is excited by the energetic particles, not by the nonlinear MHD coupling.

1 Introduction

Geodesic acoustic mode (GAM) is an oscillatory zonal flow coupled with density and pressure perturbations in toroidal plasmas[1]. In the last decade, energetic particle driven GAM (EGAM) is observed in Joint European Torus (JET), DIII-D, Large Helical Device (LHD), and HL-2A. In the DIII-D experiment, drops in neutron emission follow the EGAM bursts suggesting beam ion losses[2]. Also, in the LHD experiment, anomalous bulk ion heating during the EGAM activity suggests a GAM channeling[3]. Then, understanding EGAM is important for magnetic confinement fusion where the energetic particles need to be well confined and the bulk plasma need to be efficiently heated. The EGAM has been studied extensively. It was demonstrated that the poloidal mode number of the EGAM is 0 for potential and 1 for density. Also, the EGAM is a global mode

with the spatially uniform oscillation frequency. In addition, the EGAM frequency can be lower or higher than the conventional GAM frequency under the different conditions[4]. The above demonstrations were made theoretically, computationally, and experimentally.

Recently, in LHD, an abrupt excitation of a half-frequency secondary mode was observed when the frequency of a chirping primary EGAM reaches twice of the GAM frequency[5]. The secondary mode is important because of its low frequency. The lower frequency mode has a lower phase velocity, thus, this mode is more easily to interact with the thermal ions and to transfer energy to them. Then, the plasma heating becomes easier. Since the appearance of the secondary mode is related with the neutral beam injection (NBI), the secondary mode may create an energy channel between the energetic particles and the bulk plasmas. A 1-dimensional simulation with the kinetic energetic particles and a nonlinear coupling coefficient between the primary and secondary modes was used to reproduce these two modes, and the authors claimed that the secondary mode is driven by the cooperative combination of fluid nonlinearity and kinetic nonlinearity[6].

2 Simulation Model and Parameters

A hybrid simulation code for energetic particles interacting with a magnetohydrodynamic (MHD) fluid, MEGA[7, 8], is used for the simulation of EGAMs. In the MEGA code, the bulk plasma is described by the nonlinear MHD equations. The drift kinetic description and the δf particle method are applied to the energetic particles.

A realistic 3-dimensional equilibrium generated by HINT2 code is used for the simulation. This equilibrium data is based on the LHD shot #109031 at time t = 4.94s. At this moment, the EGAM activity is very strong, thus it is good to reproduce the EGAM phenomenon.

In the experiment of LHD, the EGAMs were observed under 2 types of energetic particle distribution. One is the slowing-down distribution, and another is the bump-on-tail distribution[3, 5]. The EGAM behaviors with these 2 distributions are similar, but the half-frequency secondary mode appears only under the condition of bump-on-tail distribution. Correspondingly, in the present work, we implement the simulation with 2 distributions. The energetic particle velocity distribution function $f(v)$ with slowing-down type is:

$$f(v) = \frac{1}{v^3 + v_c^3}, \tag{1}$$

where v_c is the critical velocity. For the bump-on-tail distribution, the charge exchange is considered, and the velocity distribution becomes:

$$g(v) = C(v^3 + v_c^3)^{\frac{1}{3}\tau_s/\tau_{cx}-1}, \tag{2}$$

where C is an integration constant, τ_s is the slowing down time, and τ_{cx} is the charge exchange time. The shape of the distribution function is controlled by the ratio of τ_s/τ_{cx}. For $\tau_{cx} \to \infty$, the τ ratio is 0 and the function is the typical slowing-down type which is the same as Eq. (1). With the increase of τ_s/τ_{cx}, the slowing down becomes insufficient gradually, and more energetic particles distribute in the high-energy region and make a

bump-on-tail distribution. In addition, a Gaussian-type pitch angle distribution $h(\Lambda)$ is assumed for the energetic ions:

$$h(\Lambda) = exp[-(\Lambda - \Lambda_{peak})^2/\Delta\Lambda^2], \tag{3}$$

where Λ_{peak} represents the pitch angle for the distribution peak and $\Delta\Lambda$ is a parameter to control the distribution width.

The parameters for the EGAM simulation are based on an LHD experiment[3], $B_0 = 1.5$ T, electron density $n_e = 0.1 \times 10^{19}$ m^{-3}, electron temperature at the magnetic axis $T_e = 4$ keV, and bulk plasma beta value on the magnetic axis equals to 7.2×10^{-4}. The injected neutral beam energy is $E_{NBI} = 170$ keV. The safety factor q value is $q = 2.82$ on the magnetic axis and $q = 0.84$ on the plasma edge, negative normal shear. The major radius of the magnetic axis is $R_0 = 3.7$ m. Cylindrical coordinates (R, ϕ, z) are employed. For LHD equilibrium, there are 10 pitches in the toroidal direction. Since the toroidal mode number of GAM is 0, for simplicity, only 1 pitch is used for the present simulation. The numbers of grid points of this pitch in (R, ϕ, z) directions are $(128, 64, 128)$, respectively.

3 Simulation Results with Slowing-Down Distribution

The EGAM is observed in LHD is reproduced by MEGA code, as shown in Fig. 1. The upper panel represents the frequency spectrum of v_θ, which is obtained by Fast Fourier Transform. The initial frequency is 55 kHz, which is similar to the LHD experiment[3, 9]. The chirping rate is about 15 kHz/ms, which is also consistent with the experiment[9]. The bottom panel represents the poloidal velocity v_θ evolution. In the linear growth phase, the mode amplitude increases with growth rate $\gamma/\omega_{EGAM} = 19\%$.

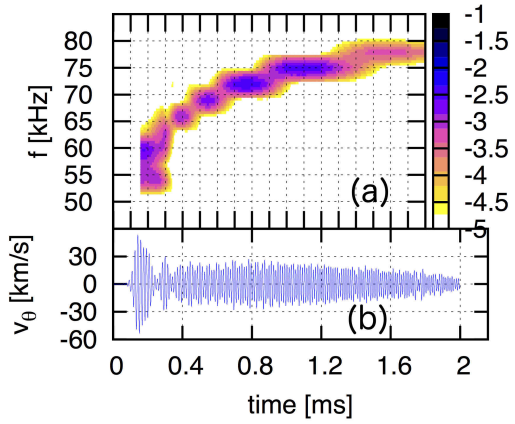

FIG. 1: The EGAM is reproduced by MEGA code. The poloidal velocity (a) frequency spectrum and (b) evolution are shown.

The mode profiles of poloidal velocity v_θ and bulk pressure perturbation δP_{bulk} are plotted in 3-dimensional figures, as shown in Fig. 2. The v_θ is plotted at t = 0.140 ms,

and the δP_{bulk} is plotted at t = 0.139 ms. The mode is already saturated at these 2 moments. The 5 slices in each panel represent 5 poloidal cross-sections, and their toroidal positions are from $\phi = 0$ to $\phi = 0.4\pi$ with toroidal interval of 0.1π. For v_θ, the blue color represents positive value, in other words, it represents the counter-clockwise rotation in poloidal direction, while the red color represents the clockwise rotation. For δP_{bulk}, the blue color represents positive perturbation while the red is negative perturbation. The poloidal velocity v_θ is a combination of $m/n = 0/0$, $1/0$ and $2/10$ components, and the δP_{bulk} is a combination of $m/n = 1/0$ and $2/0$. The relation between different components are quantitatively shown in Fig. 3 in a 2-dimensional form. In Fig. 3(a), the most dominant 3 harmonics are $m/n = 0/0$, $1/0$ and $2/10$, and other components are negligible. The amplitude of the $2/10$ component is 17% of the $0/0$ component. The $m/n = 2/10$ components exists due to the LHD configuration. In LHD, there are 10 pitches in the toroidal direction, and there are 2 high field regions and 2 low field regions in the poloidal direction. This is the first simulation of EGAM in the 3-dimensional LHD configuration. The mode number is different from the tokamak case, where the v_θ oscillation is a combination of $m/n = 0/0$ and $1/0$ components. In the present work, the dominant mode number of pressure perturbation is $m/n = 1/0$ and $2/0$. The pressure perturbation rotates poloidally in the nonlinear saturated phase, and the rotation direction changes periodically. This rotation is caused by the convection of EGAM. Also, it is found that the mode doesn't radially propagate in the linear phase, but propagates inward in the nonlinear saturated phase.

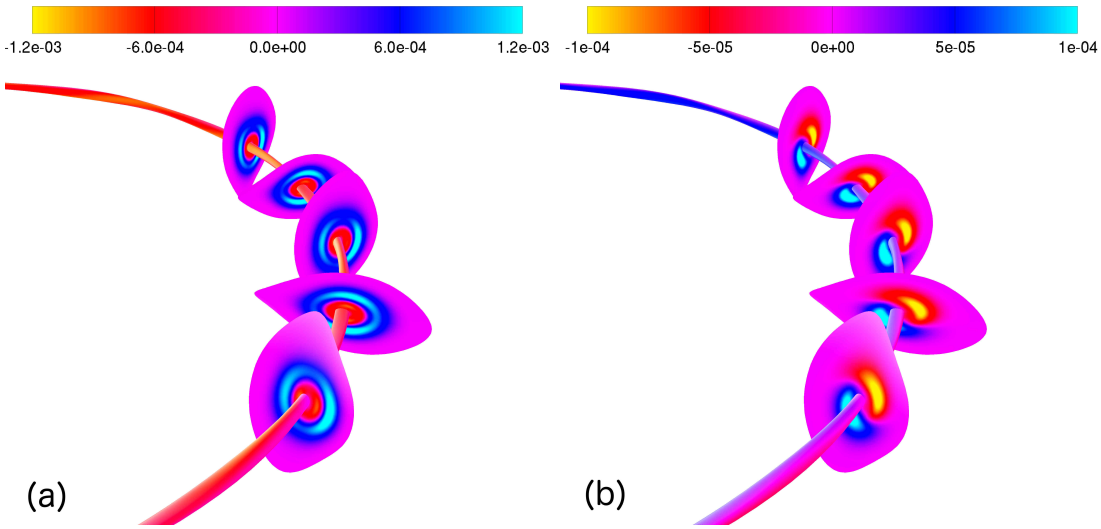

FIG. 2: The mode profiles of (a) v_θ and (b) δP_{bulk} in the 3-dimensional form.

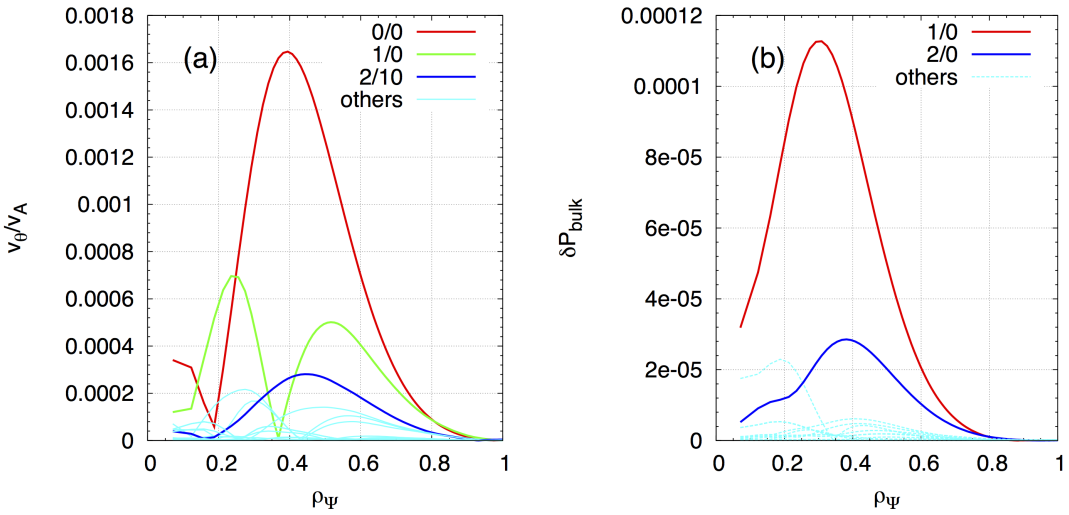

FIG. 3: The mode profiles of (a) v_θ and (b) δP_{bulk} in the 2-dimensional form.

4 Simulation Results with Bump-On-Tail Distribution

Both the chirping primary mode and the half-frequency secondary mode are reproduced by the MEGA code, as shown in Fig. 4. Figure 4(a) shows the poloidal velocity v_θ frequency spectrum, and Fig. 4(b) shows v_θ evolution. The primary mode frequency chirps from 70 kHz. The mode is saturated at $t = 0.07$ ms, and then, steps into the nonlinear phase. At $t = 1.1$ ms, the frequency of the primary mode reaches to 96 kHz, and a secondary mode with frequency $f = 48$ kHz is excited. The simulated phenomenon is very similar to the experimental observation, as shown in Fig. 2 of Ref. [5]. In addition, the mode profile of v_θ and δP_{bulk} are analyzed, the mode numbers are same as experimental measurements. Also, the modes are global for both the simulation and experiment. Figure 4(c) shows the Lissajous curves in order to demonstrate the phase lock between the primary mode and the secondary mode. The frequency relation between these modes are double. The Lissajous curves are similar with the experimental measurements[5]. The above comparisons between simulation and experiment show a very good code validation. This is the first time to reproduce both the primary mode and secondary mode with 3-dimensional model and realistic input parameters.

The secondary mode is identified as an EGAM in the present work, because of 3 reasons. Firstly, the poloidal mode number is $m = 0$ for poloidal velocity and $m = 1$ for density. This is the feature of the EGAM and the conventional GAM. Secondly, the mode frequency is almost same as the conventional GAM frequency, but slightly lower. According to the theoretical prediction, under the present simulation conditions, the conventional GAM frequency should be 50.1 kHz. The simulated frequency of the secondary mode is 48 ± 1.5 kHz. In Ref. [4], the EGAM frequency can be lower than the conventional GAM frequency, thus the simulated secondary mode may be a kind of EGAM. Thirdly,

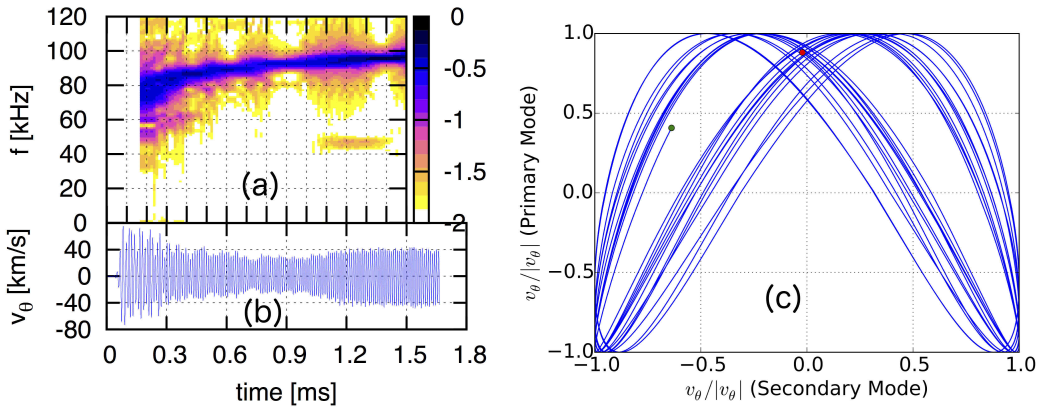

FIG. 4: The EGAMs are reproduced by MEGA code. Figures (a), (b) and (c) show the poloidal velocity frequency spectrum, evolution, and Lissajous curves, respectively.

the secondary mode is global. The EGAM is global while the conventional GAM is local, and this is one of the differences between the EGAM and the conventional GAM[4]. Based on the above 3 properties, we conclude that the simulated secondary mode is an EGAM.

In order to investigate the reason why the frequency of secondary mode is lower than the primary mode, the bulk plasma pressure perturbation δP_{bulk} and the energetic particle pressure perturbation $\delta P_{h\|}$ are analyzed, as shown in Fig. 5. The most dominant components of v_θ, δP_{bulk} and $\delta P_{h\|}$ are $m/n = 0/0$ cosine, $m/n = 1/0$ sine, and $m/n = 1/0$ sine, respectively. In the figure, for simplicity, only these 3 most dominant components are shown. Since the pressure perturbation is much weaker than the poloidal velocity perturbation, a factor 10 is considered for pressure to make an intuitional comparison. For the primary mode, the phase of δP_{bulk} and $\delta P_{h\|}$ are the same. Compared with v_θ, the phase of pressure is 0.5π earlier. The primary mode is driven by both δP_{bulk} and $\delta P_{h\|}$. For the secondary mode, the phase differences between δP_{bulk} and $\delta P_{h\|}$ is π. They cancel out with each other. Thus, the frequency of the secondary mode is much lower than the primary mode. The phase of $\delta P_{h\perp}$ is same as $\delta P_{h\|}$, but the absolute value of $\delta P_{h\perp}$ is smaller, so $\delta P_{h\perp}$ is not shown in the figure.

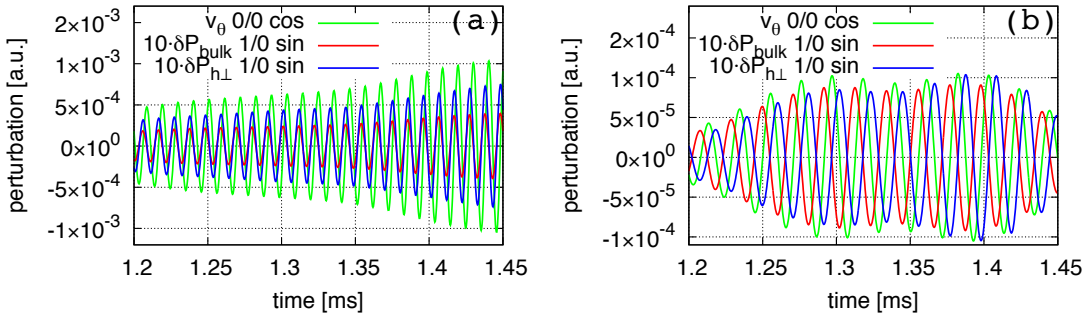

FIG. 5: The v_θ, δP_{bulk} and $\delta P_{h\|}$ oscillation of (a) primary mode and (b) secondary mode.

In Ref. [6], the authors claimed that both the fluid nonlinearity and the kinetic nonlin-

earity are important for the secondary mode excitation. In order to clarify the importance of the fluid nonlinearity, a special linear MHD model is applied. The linear MHD equations are same as that in Ref. [7]. In the present work, simulations are run in 2 steps. In the 1st step, the nonlinear code is run, until time t = 0.97 ms when the EGAM is completely saturated but the secondary mode has not been excited yet. Then, in the 2nd step, both the linear and nonlinear MHD codes are run separately from the end of the run of the 1st step. In the 2nd step, the secondary mode appears in both runs. In other words, the secondary mode can be excited even if the MHD equations are linearised. This result is different from that in Ref. [6]. In the present work, the excitation of the secondary mode is only caused by the kinetic nonlinearity, while the fluid nonlinearity hardly works. In order to clarity the role of the kinetic nonlinearity, the resonate particles are analyzed, as shown in Fig. 6. The 32 particles whose δf values are the largest among all the particles are analyzed in the linear phase and in the moment when the activity of the secondary mode is very strong. In the figure, ω is the primary mode frequency, and ω_θ is the transit frequency of the resonate particle. In the linear phase, the mode frequency is 70 kHz, and many particles are located at ω/ω_θ = -1. In other words, most resonate particles' transit frequencies are the same as the mode frequency. In addition, some particles are located at ω/ω_θ = 2, or $\omega_\theta/(2\pi)$ = 35 kHz. During the activity of the secondary mode, apparently, most resonant particles are located at ω/ω_θ = 2, or $\omega_\theta/(2\pi)$ = 50 kHz. The particles transit frequencies are the same as the secondary mode frequency. It indicates that the secondary mode may be excited by the resonant particles. Similar with Ref. [8], we have the resonance condition $\omega_1 = l_1\omega_\theta$ and $\omega_2 = l_2\omega_\theta$, where the subscript 1 denotes the primary mode, the subscript 2 denotes the secondary mode, and l is an arbitrary integer. When the primary mode frequency chirps up to 100 kHz, the particles with $\omega_\theta/(2\pi)$ = 50 kHz resonate with both the primary and the secondary modes for l_1 = 2 and l_2 = 1, respectively. Energy of the primary mode may be transferred to the secondary mode through the resonant particles leading to the excitation of the secondary mode. Further investigation will be implemented soon to clarify the detailed mechanism.

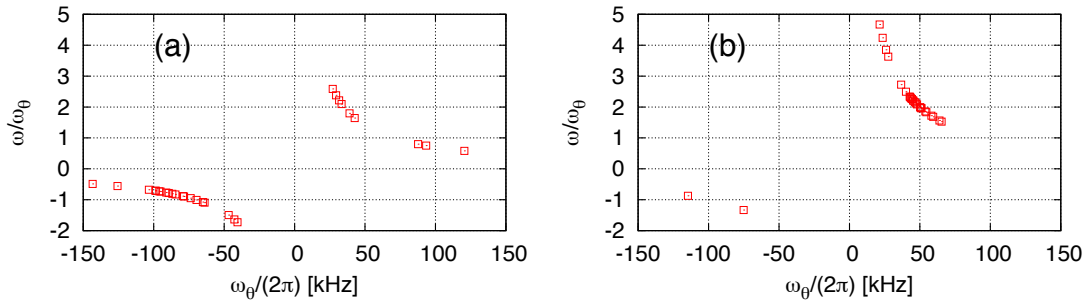

FIG. 6: The 32 particles whose δf values are the largest among all the particles are analyzed in (a) the linear phase and in (b) the moment when the activity of the secondary mode is very strong.

5 Summary and Conclusions

In summary, 3 conclusions are obtained in the present work. Firstly, the simulation of EGAM in the realistic 3-dimensional equilibrium is obtained for the first time, and the results are very similar to the experimental observation. It is found that the poloidal velocity oscillation is a combination of $m/n = 0/0$ (strong), 1/0 (medium) and 2/10 (weak) components. This is different from the tokamak case. Secondly, the chirping EGAM and the associated secondary mode are reproduced with the 3-dimensional model and realistic parameters for the first time. The results are good validations of the simulation. It is found that the phase differences between δP_{bulk} and $\delta P_{h\|}$ is π for the secondary mode. The δP_{bulk} and $\delta P_{h\|}$ cancel out with each other, and thus, the frequency of the secondary mode is much lower than the primary mode. Thirdly, it is found that the fluid nonlinearity doesn't work for the excitation of the secondary mode, which is different from the conclusion of Ref. [6]. The secondary mode may be excited by the resonant particles, whose transit frequencies are the half of the primary mode frequency.

References

[1] DIAMOND, P.H., et al., "Zonal flows in plasma a review", Plasma Phys. Controlled Fusion **47** (2005) R35.

[2] NAZIKIAN, R., et al., "Intense Geodesic Acousticlike Modes Driven by Suprathermal Ions in a Tokamak Plasma", Phys. Rev. Lett. **101** (2008) 185001.

[3] OSAKABE, M., et al., "Indication of bulk-ion heating by energetic particle driven Geodesic Acoustic Modes on LHD", paper number EX/10-3, IAEA-FEC, St. Pertersburg (2014).

[4] FU, G. Y., "Energetic-Particle-Induced Geodesic Acoustic Mode", Phys. Rev. Lett. **101** (2008) 185002.

[5] IDO, T., et al., "Strong Destabilization of Stable Modes with a Half-Frequency Associated with Chirping Geodesic Acoustic Modes in the Large Helical Device", Phys. Rev. Lett. **116** (2016) 015002.

[6] LESUR, M., et al., "Nonlinear Excitation of Subcritical Instabilities in a Toroidal Plasma", Phys. Rev. Lett. **116** (2016) 015003.

[7] TODO, Y., et al., "Nonlinear magnetohydrodynamic effects on Alfvén eigenmode evolution and zonal flow generation", Nucl. Fusion, **50** (2010) 084016.

[8] WANG, H., et al., "Simulation study of high-frequency energetic particle driven geodesic acoustic mode", Phys. Plasmas, **22** (2015) 092507.

[9] IDO, T., et al., "Identification of the energetic-particle driven GAM in the LHD", Nucl. Fusion **55** (2015) 083024.